Optimum Part Build Orientation in Additive Manufacturing for Minimizing Part Errors and Support Structures

Paramita Das, Ramya Chandran, Rutuja Samant and Sam Anand

Department of Mechanical and Materials Engineering
Center for Global Design and Manufacturing
University of Cincinnati, Cincinnati, OH 45221
daspa@mail.uc.edu, chandrry@mail.uc.edu, samantrv@mail.uc.edu, sam.anand@.uc.edu

Abstract

Additive Manufacturing (AM) is the process of part building by stacking layers of material on top of each other. Various challenges for a metal powder based process include reducing the staircase effect which leads to poor surface finish of the part, and minimal use of support structures for regions with overhangs or internal hollow volumes. Part build orientation is a crucial process parameter which affects part quality, in particular, Geometric Dimensioning & Tolerancing (GD&T) errors on the part, the energy expended and the extent of support structures required. This paper provides an approach to identify an optimal build orientation which will minimize the volume of support structures while meeting the specified GD&T criteria of the part for a DMLS based process. Siemens PLM NX API is used to extract the GD&T callouts and associated geometric information of the CAD model. The regions requiring support structures are identified and a Quadtree decomposition is used to find the volume of support structures. The mathematical relationships between build orientation and GD&T are developed as part of a combined optimization model to identify best build orientations for minimizing support structures while meeting the design tolerances. The feasible build orientations along with the corresponding support structures are depicted using a visual model.

Keywords: Additive Manufacturing, Build Orientation, Support Structures, Geometric Tolerances, Optimization, Feasible Zone, Siemens PLM NX API, Quadtree.

1 Introduction

Metal powder based Additive Manufacturing is gaining popularity in the aerospace, medical, electronics and automobile industry, as intricate components can be built with ease. The process begins by slicing the CAD model to obtain a 2D contour at each level of the build axis, which is fixed

as the z-axis. Starting from the base 2D contour, a user defined slice thickness is added cumulatively at successive slicing planes. This layer by layer stacking gives rise to an error called the staircase effect which diminishes the surface finish of the part. Achieving part accuracy is currently one of the key constraints in AM. Slice thickness, part build orientation, thermal errors, support structures are a few major parameters which affect part accuracy. In this paper, the effect of part build orientation on support structures volume and part accuracy will be addressed.

Build orientation is a crucial parameter since it will affect the tolerance errors, energy expended and the volume of support structures required. Support structures are an integral part of this process as it is necessary to account for possible overhangs or internal hollow volumes which might not provide sufficient support to the overhanging layers. It is essential to minimize the use of these supports as reduced contact area between the part and these structures will result in better part quality and also reduce the post processing efforts (Dutta and Kulkarni, 2000).

This paper discusses a methodology to detect the regions requiring support and calculate the volume of these support structures at various orientations. This information is then used to find an optimal build orientation, having minimum support structures while satisfying the tolerance callouts.

The tolerances covered in this paper are Perpendicularity, Parallelism, Angularity, Total Runout, Circular Runout and Conicity. Assuming a fixed slice thickness, mathematical relations are developed between the tolerance errors and part orientation. A combined optimization model is used to obtain the optimal build angle which is then verified using the graphical representation adapted from Arni and Gupta (Arni and Gupta, 2001) and Paul and Anand (Paul and Anand, 2014). Finally, the volume of support structures at different orientations is plotted on a unit sphere depicting different build orientations which can act as a tool for visualizing and comparing extent of supports. A combined visual representation of volume of support structures and the tolerances satisfied at each orientation is also presented.

2   Literature Review

Process parameters play an important role in defining the final part quality and part accuracy of a product. In additive manufacturing, these parameters include slice thickness, build orientation, support structures and hatching pattern. Literature review on support structures, optimal part build orientation, and GD&T errors, namely, form and orientation tolerance errors and their evaluation is discussed here.

Dutta and Kulkarni (Dutta and Kulkarni, 2000) covered the various process planning parameters of AM and included part orientation and support structure among the important factors. They also enumerated the various approaches to solve the support structure and build orientation problems. Prior research includes the use of various algorithms to determine optimal part orientation with respect to build time, volumetric error, part accuracy, surface finish and build cost (Cheng et al., 1995, Thrimurthulu et al., 2004, Frank and Fadel, 1995, Rattanawong, et al., 2001, Thompson and Crawford, 1997, Pandey et al., 2004, Xu et al., 1997, Alexander et al., 1998, Lan et al., 1997 and Zhang and Li, 2013). Arni and Gupta (Arni and Gupta, 2001) investigated the effect of build orientation on flatness error and analyzed the feasibility of manufacturing the part with flatness callout. They concluded that the staircase error formed due to slice thickness and build orientation is the cause of the flatness error on the manufactured part and established a mathematical relation between them. Lynn-Charney and Rosen (Lynn-Charney and Rosen, 2000) developed an empirical model for SLA machine accuracy and established relationships among part surfaces, tolerances and process variables. Other researchers (Prakasvudhisarn and Raman, 2004, Wen et al., 2010) performed detailed analysis and evaluated conicity and cylindricity errors using different optimization techniques. Paul and Anand (Paul and Anand, 2014) analyzed the effect of build orientation on cylindricity error and developed an optimization model to obtain the part orientation while minimizing support structures and form errors. They also introduced a graphical approach to find the optimal build orientation. Allen and Dutta

(Allen and Dutta, 1994) have used ray structures and convex hulls to find the best orientation from a candidate list or orientations. The selection criterion for orientation is based on minimization of contact area between the part and the supports. Majhi et al. (Majhi et al., 1999) used computational geometry to minimize the area of support structures and the contact length with the part. They also tried to minimize the volume of trapped volumes for convex polyhedrons. An extension of this by Majhi et al. (Majhi et al., 1998) includes minimization of degree of stair stepping for any part and geometric formulations for optimized support volumes for simple, non-convex parts. Yang et al. (Yang, et al., 2003) have used the difference in area of successive layers for a multi-orientation deposition method to minimize the use of support structures. This paper presents a Quadtree based approach for the calculation of support structure volumes. Related work using Quadtree for border and image representation have been performed by (Dyer et al., 1980), (Samet and Tamminen, 1985) and (Samet, 1980).

The combined effect of part errors and the volume of support structures on obtaining the optimal part orientation has never been analyzed before. This paper explains in detail the methodology for the combined optimization to find the build orientation with minimal supports while satisfying the form and orientation tolerance callouts.

3 Methodology

This section presents the various steps that are involved in building the final optimization model. The first section explains the Product Manufacturing Information (PMI) extraction from a NX part model which is later used in the optimization routine to obtain the optimal build angle. Relationship between tolerance errors and part build orientation is discussed in the next section followed by determining the volume of support structures at the optimal orientation.

An overview of the steps that will be followed in the paper is:
- Extract the GD&T callouts and the normal of face or axis of non-planar feature from the CAD model using Siemens PLM NX API.
- Establish mathematical relations between part orientation and tolerance errors and calculate tolerance error values using the extracted normal/axis information of the CAD model.
- Discretize the CAD model and using the normal information, detect regions requiring support. Use a Quadtree approach to calculate the volume of support structures required.
- The GD&T callouts extracted from the CAD model and the volume of supports serves as an input to the optimization model to obtain the optimal build orientation.
- Verify the obtained optimal build angle using the graphical approach.
- Present a combined visual representation of volume of supports and corresponding tolerances at different orientations on a unit sphere.

3.1 Product Manufacturing Information (PMI) Extraction from the CAD model using Siemens PLM NX API

PMI is the way of representing non-geometric attributes in a 3D CAD model essential for manufacturing the part. It consists of GD&Ts, annotations, surface finish and material specifications (Siemens PLM Software, 2009). In this paper, GD&T callouts of the given part are extracted along with the normal information of the face, or axis information of the non-planar feature associated with each GD&T specification using Siemens PLM NX Application Programming Interface (API). The normal and axis information is later used to map the build orientation to tolerance errors. The errors are then compared with the extracted GD&T callouts which shows if a part has met the GD&T criteria or not.

The CAD model considered to demonstrate the PMI extraction has Perpendicularity, Parallelism, Angularity, Cylindricity and Flatness tolerance associated with it as shown in Figure 1. All the required information is extracted using Siemens PLM NX API as shown in Figure 2.
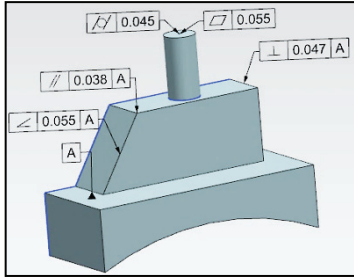

Figure 1: Sample CAD model with tolerance callouts

Information is displayed only concerning the faces or features associated with GD&T callouts. The "type" in Figure 2 represents the type of surface, e.g. 22 stands for planar surface, 16 stands for cylindrical feature. Depending on the "type", the "dir" either gives the normal vector of the face or the axis vector of the cylinder. The angle of the normal of the face or the axis of the cylinder with the build axis (z-axis) is stored in the variable "degree". The "characteristic" gives the name of the tolerance associated with the face or feature, e.g. charateristic1 is flatness. The tolerance value associated with it is stored in "Item Value", e.g.

Name	Value
faceTag1	36941
type	22
dir	0x000000000022d9f8
[0]	0.00000000000000000
[1]	0.00000000000000000
[2]	1.0000000000000000
degree	0.00000000000000000
characteristic1	FcfCharacteristicFlatness
tolerance1	{ItemValue=0.0550000000000003
ItemValue	0.0420000000000003
ValueExpression	0x0000000000000000 {m_expression
ValuePrecision	3
faceTag2	36932
type2	16
dir2	0x000000000022dab8
[0]	-0.00000000000000000
[1]	-0.00000000000000000
[2]	-1.0000000000000000
degree2	-2.0567998149090272e-007
characteristic2	FcfCharacteristicCylindricity
tolerance2	{ItemValue=0.0450000000000003

Figure 2: Part information extracted using Siemens PLM NX API

0.055 for Flatness. This extracted information is later utilized to calculate the tolerance errors in the optimization function to obtain the optimal build angle.

3.2 Relation between Tolerance Errors and Build Orientation

Arni and Gupta (Arni and Gupta, 2001) established the relation between Flatness error ($\mathcal{E}_f$) for a nominal flat feature and build orientation as given in equation 1,

$$\mathcal{E}_f = \Delta z \cos (\Theta_f) \quad\text{.. (1)}$$

where, Δz is the slice thickness, Θ_f is the angle between the normal of the face with flatness tolerance and z axis. Relationship between Cylindricity error ($\mathcal{E}_{cyl}$) and build orientation was addressed by Paul (Paul, 2013) and Paul and Anand (Paul and Anand, 2014) as shown in equation 2,

$$\mathcal{E}_{cyl} = \Delta z \sin (\Theta_{cyl}) \quad\text{.. (2)}$$

where, Θ_{cyl} is the angle between the axis of the cylinder with cylindricity tolerance and build direction.

In this paper, the relations established by Arni and Gupta (Arni and Gupta, 2001) and Paul and Anand (Paul and Anand, 2014), have been extended for the Orientation tolerances (Perpendicularity, Parallelism and Angularity), Runout tolerances (Total Runout and Circular Runout) and Conicity.

The *Perpendicularity error* ($\mathcal{E}_{per}$) by definition is the minimum tolerance zone between two parallel planes perpendicular to a datum plane or axis, within which all the points sampled from the manufactured part must lie (ASME, 1994). As seen from Figure 3, when a part is manufactured in a particular orientation, in slices, additional material gets deposited on each layer, producing a staircase effect. This generates two parallel planes which contains all the
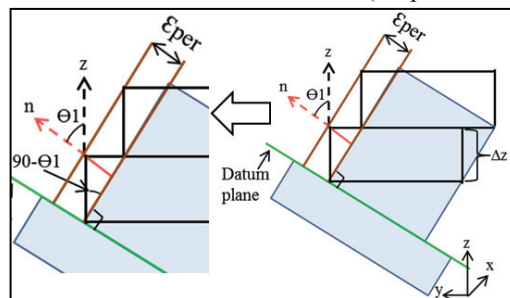

Figure 3: Perpendicularity Error

manufactured points of the part. An added constraint is that these parallel planes should also be perpendicular to the datum plane. The perpendicularity tolerance is given by equation 3 as,

$$\varepsilon_{per} = \Delta z \cos (\Theta_{per}) \ldots\ldots\ldots (3)$$

where, Θ_{per} is the angle between the normal of the face with perpendicularity tolerance and z axis.

Similarly, *Parallelism error* (ε_{para}) as defined by ASME is the minimum tolerance zone between two parallel planes which are parallel to a datum plane or axis and contains all the points sampled from the manufactured part (ASME, 1994). As shown in Figure 4, the Parallelism error (ε_{para}) is,

$$\varepsilon_{para} = \Delta z \cos (\Theta_{para}) \ldots\ldots\ldots\ldots (4)$$

Figure 4: Parallelism Error

where, Θ_{para} is the angle between the normal of the face with parallelism tolerance and z axis.

Angularity error (ε_{ang}) is defined by ASME as the minimum tolerance zone between two parallel planes at a specified angle (other than 0° or 90°) to the datum plane and containing the points sampled from the manufactured feature (ASME, 1994). Thus, as shown in Figure 5, Angularity error (ε_{ang}) is given by equation 5,

$$\varepsilon_{ang} = \Delta z \cos (\Theta_{ang}) \ldots\ldots\ldots\ldots (5)$$

where, Θ_{ang} is the angle between the normal of the face with angularity tolerance and z axis.

Figure 5: Angularity Error

Conicity error (ε_{con}) is defined as the radial distance between two cones having same basic angle and containing all the manufactured points (Wen et al., 2010). This radial distance is illustrated in the Figure 6. Conicity error can be written as,

$$\varepsilon_{con} = \Delta z \cos (\Theta_{cone} + \alpha) \ldots\ldots\ldots (6)$$

where, Θ_{cone} is the angle between the axis of the cone and z axis, α = basic angle of the cone.

For a feature constructed around a datum axis, the *Total Runout error* (ε_{tot_runout}) is the measure of the total deviation of the entire surface for that particular feature from the datum axis (Paul, 2013), (Ramaswami et al., 2011). Figure 7 shows the Total Runout error. It is the distance between the farthest manufactured point from the datum axis and the nearest manufactured point from the datum axis and can be given by the following relation,

$$\varepsilon_{tot\_runout} = r1 + \Delta z \sin (\Theta_{tot\_runout}) - r1 = \Delta z \sin (\Theta_{tot\_runout}) \ldots\ldots\ldots (7)$$

where, Θ_{tot_runout} is the angle between the datum axis and z axis.

Circular Runout error (ε_{cir_runout}) determines the deviation of a feature at a certain cross section, normal to the datum axis (Ramaswami et al., 2011), (Paul, 2013) as seen in Figure 8. The cross section is assumed to be of very small thickness.

$$\varepsilon_{cir\_runout} = \Delta z \sin (\Theta_{cir\_runout}) \ldots\ldots\ldots\ldots\ldots (8)$$

where, Θ_{cir_runout} is the angle between the datum axis and z axis.
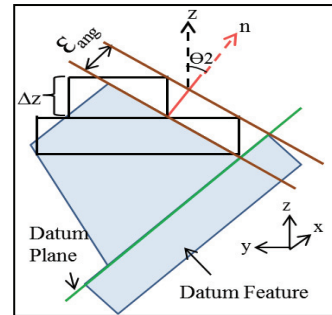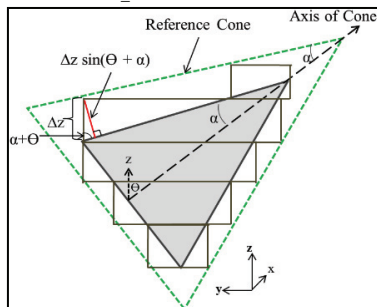

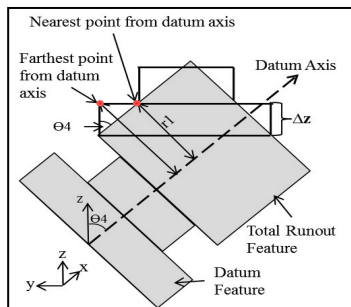Figure 6: Conicity Error

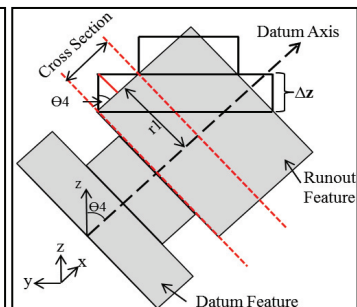Figure 7: Total Runout Error

Figure 8: Circular Runout Error

347

3.3 Mapping of Build Orientations for the Errors

This section extends Paul (Paul, 2013) and Paul and Anand's (Paul and Anand, 2014) one dimensional tolerance maps to orientation tolerances. Assuming that a given AM part feature has a perpendicularity tolerance specification ($\mathcal{E}_{sp\_per}$), a parallelism tolerance specification ($\mathcal{E}_{sp\_para}$) and an angularity tolerance specification of ($\mathcal{E}_{sp\_ang}$), then for a fixed slice thickness, there exists two orientations where the tolerance errors will be exactly same as the specified callout, as depicted in equations 9, 10 and 11.

$$\theta_{cr1} = \cos^{-1}(\frac{\varepsilon_{sp\_per}}{\Delta z}) \,, \ \theta_{cr2} = 180 - \theta_{cr1} \ \dots\dots\dots\dots\dots\dots \ (9)$$

$$\theta_{cr3} = \cos^{-1}(\frac{\varepsilon_{sp\_para}}{\Delta z}) \,, \ \theta_{cr4} = 180 - \theta_{cr3} \ \dots\dots\dots\dots\dots \ (10)$$

$$\theta_{cr5} = \cos^{-1}(\frac{\varepsilon_{sp\_ang}}{\Delta z}) \,, \ \theta_{cr6} = 180 - \theta_{cr5} \ \dots\dots\dots\dots\dots \ (11)$$

As seen from the above equations, the tolerances of the manufactured part will be met provided the normal of the face associated with the particular tolerance lies within the θ_{cr} range as shown in equations 12, 13 and 14.

$$\theta_{cr1} \leq \theta_{per} \leq \theta_{cr2} \ \dots\dots\dots\dots\dots\dots\dots\dots\dots\dots\dots\dots \ (12)$$

$$\theta_{cr3} \leq \theta_{para} \leq \theta_{cr4} \ \dots\dots\dots\dots\dots\dots\dots\dots\dots\dots\dots\dots \ (13)$$

$$\theta_{cr5} \leq \theta_{ang} \leq \theta_{cr6} \ \dots\dots\dots\dots\dots\dots\dots\dots\dots\dots\dots\dots \ (14)$$

The critical range of $\Theta_{cr1}, \Theta_{cr2}, \Theta_{cr3}, \Theta_{cr4}, \Theta_{cr5}, \Theta_{cr6}$ is called the feasibility range or feasibility zone for the particular build orientation.

Paul and Anand mapped the cylindricity and flatness errors to a 1D line space and developed a combined error function (Paul and Anand, 2014). The penalty for cylindricity error and flatness error associated with the mth feature with cylindricity tolerance and n[th] feature with flatness tolerance of a part is given by equations 15 and 16.

$$p_{cyl} = 1 - (c_z^2)_{cyl}^m \ \dots\dots\dots\dots \ (15) \qquad p_{flat} = (c_z^2)_{flat}^n \ \dots\dots\dots\dots \ (16)$$

where, p_{cyl} and p_{flat} is the penalty for cylindricity error and flatness error.

A similar approach is followed for perpendicularity, parallelism and angularity errors. Consider a part having n_{per} critical perpendicular features with ε_{sp_per} as the user specified perpendicularity tolerance callout, n_{para} critical parallel features with ε_{sp_para} as the parallelism tolerance callout and n_{ang} critical angular features with ε_{sp_ang} as the angularity tolerance callout. $\gamma_{per,para,ang}^i$ is the angle which the normal of the ith perpendicular face or parallel face or the angular face makes with the build direction, i.e. z axis respectively. Keeping the slice thickness fixed, the tolerance errors will be satisfied if the angle $\gamma_{per,para,ang}^i$ lies within the critical zones as shown in equation 17.

$$(\gamma_{crj})_{per,para,ang}^i \leq \gamma_{per,para,ang}^i \leq (\gamma_{crk})_{per,para,ang}^i \ \dots\dots\dots\dots\dots\dots \ (17)$$

where $(\gamma_{crj})_{per,para,ang}^i$ and $(\gamma_{crj})_{per,para,ang}^i$ is the lower and upper critical angle of the feasibility zone for the ith perpendicularity, parallelism and angularity tolerance feature respectively. However,

$$(\gamma_{crk})_{per,para,ang}^i = 180 - (\gamma_{crj})_{per,para,ang}^i \ \dots\dots\dots\dots\dots\dots\dots\dots \ (18)$$

$$\Rightarrow (\gamma_{crj})_{per,para,ang}^i \leq \gamma_{per,para,ang}^i \leq 180 - (\gamma_{crj})_{per,para,ang}^i \ \dots\dots\dots\dots \ (19)$$

Taking squares of cosines on both sides of the equation 19 gives,

$$0 \leq (c_z^2)_{per,para,ang}^i \leq (c_{crj}^2)_{per,para,ang}^i \ \dots\dots\dots\dots\dots\dots\dots\dots\dots\dots \ (20)$$

where c is cos (ɣ) and $(c_z^2)_{per,para,ang}^i$ is the z-component of unit normal of the ith feature with perpendicularity, parallelism and angularity tolerance respectively. Thus, for tolerances to be satisfied, the square of the z-component of the normal of the planar feature should lie between 0 and the square of the cosine of the lower critical angle for that feature. The feasible and infeasible zones for perpendicularity on a 1D line is shown in Figure 9. A penalty function can be generated if the tolerance is not satisfied based on the 1D mapping. The penalty (p_{per}) associated with the perpendicularity error of the ith feature of a part is given by equation 21 and shown in Figure 10,

$$p_{per} = (c_z^2)_{per}^i \ \dots\dots\dots\dots\dots\dots\dots\dots\dots\dots\dots\dots\dots\dots\dots\dots\dots \ (21)$$

Applying the same procedure for Parallelism and Angularity tolerance, the corresponding penalties obtained are as shown in equation 22.
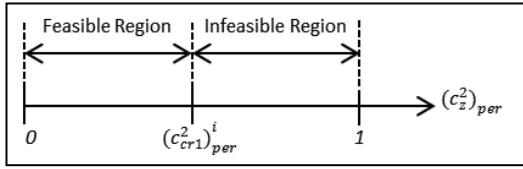

Figure 9: 1D Feasibility Zones for Perpendicularity Error (Adapted from Paul and Anand, 2014)
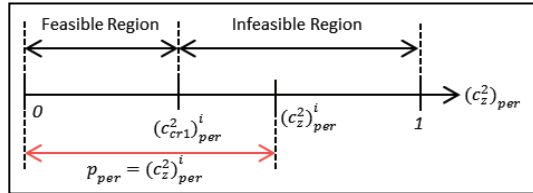

Figure 10: Penalty function for Perpendicularity tolerance (Adapted from Paul and Anand, 2014)

$$p_{para,ang} = (c_z^2)^i_{para,ang} \dots\dots\dots\dots\dots\dots\dots\dots\dots\dots\dots\dots\dots\dots\dots\dots\dots\dots (22)$$

The penalties obtained from the above relations are one of the inputs to the combined optimization model that will be presented in section 3.5.

3.4 Calculation of Volume of Support Structures

As the main aim of this paper is to find feasible build orientations with minimum support structures and tolerance errors, this section explains the methodology for calculating support structure volumes with the use of a point Quadtree (Samet, 1984). The NURBS surface of the part model is initially discretized into fine points and the normal information at these points is extracted from the CAD model using NX API. These normals are then used to calculate the angle which the surface makes with the build direction by calculating the dot product between them (Dutta and Kulkarni, 2000). It is assumed that faces of the part whose normals make 35° or less (Cloots et al., 2013) with the build direction need support structures for building them.
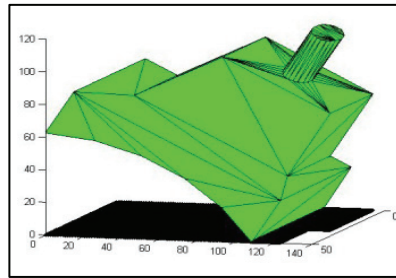

Figure 11: 2D Point cloud denoting regions requiring Support Structures

Next, only those points which pass the above criteria are projected onto the X-Y plane. The plot of this finely discretized, dense black point cloud with the considered part is shown in Figure 11.

The origin of each of these projected points is known, since they are projected from the CAD surface. These points are then used to build a point Quadtree. A Quadtree is a hierarchical data structure where a universal node is recursively divided into four equal quadrants until a termination condition is reached (Samet, 1984). A basic Quadtr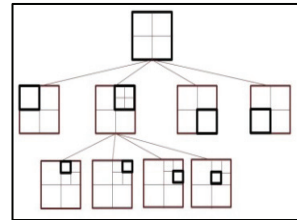ee decomposition is shown in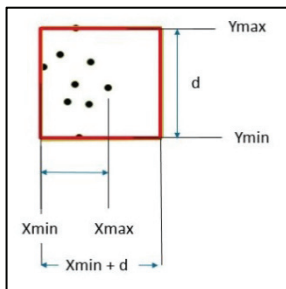 Figure 12. The universal node is the first and largest node which encloses the entire data set to be analyzed. The first division will result into 4 child nodes which are represented by the 4 quadrants highlighted in black in Figure 12.

Figure 12: Basic Quadtree Decomposition

The process of Quadtree building starts with the building of the Universal node, which in our case is an axis aligned bounding box as shown in Figure 13 in red, which encloses the 2D points projected from the CAD surface on to the XY plane. Based on the greater of the maximum 'y' distance and maximum 'x' distance of the total projected points, the length of the side of the square bounding box is fixed as 'd'.

Figure 13: Axis Aligned Bounding Box

Lines parallel to axes are constructed through the corresponding extreme points (Ymin and Ymax in

this case). Lines having length 'd' are constructed parallel to Y axis at Xmin and (Xmin +d) and the resultant Axis Aligned Bounding Box.

3.3.1 Quadtree Building

The methodology for the determination of support structures is explained in this section. It is assumed that the universal node is a gray node and is divided into four quadrants. Each of the quadrants is checked for points contained in them by the Range Search Algorithm (RSA) (Knuth, 1975). The RSA is a simple algorithm where the 'x' co-ordinates and 'y' co-ordinates of the points in the bounding box are checked to lie within the 'x' co-ordinates and 'y' co-ordinates of the parent node.

The Quadtree decomposition is performed breadth first, so if a node is found to be gray, the next sibling node is checked before diving deep into the child node of that parent. Thus, the division occurs in such a way that every node at a particular level of division is checked for points before going to the next level. Information such as the co-ordinates and the height from the substrate level of the points contained in a particular node, along with the area of the node in which it is contained is stored. If a node contains no points, it is labeled a 'white node' and is considered as a leaf node and not divided any further. This process of checking for points and dividing into quadrants continues until a pre-defined value of threshold is met and labeled as black nodes. The depth bound of the Quadtree is established when the area of the node at that level is less than or equal to 0.01% of the area of the root node. These terminal black nodes are the only nodes which contain the projected points which require supports. The Quadtree decomposition of the point plot for the test part requiring support structures at an inclination of 30^0 with the Y-axis is shown in Figure 14. As can been seen from the figure, the smallest divisions are the terminal nodes. The volume of support structures would mathematically be the sum of the areas of these terminal nodes times their corresponding heights, which is known from the CAD data point from which the projection was generated. Since there may be more than one point in each terminal node, the mean height of all these points will be assigned as the height for that corresponding node. Each of these terminal nodes are then raised by the heights assigned to them and the support structures volume plot obtained can be observed from Figure 15. Next, a multi-objective function is developed which gives the optimal build orientation which will satisfy all the GD&T callouts of the part with minimal support structure volume.
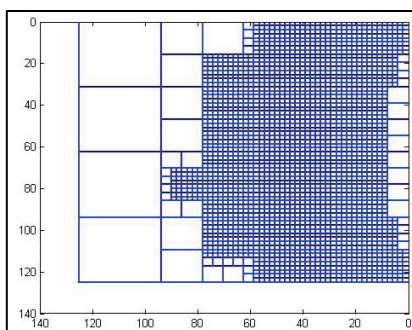

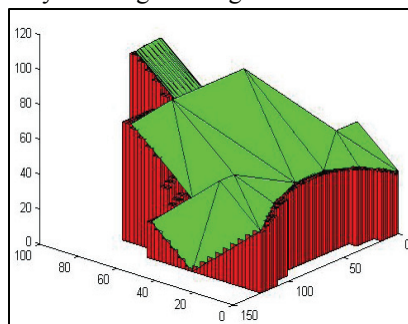Figure 14: Quadtree Decomposition of the Test Part

Figure 15: Part with required Support Structures

3.4.1 Normalization of Volume of Supports

The volume of support structure at each orientation after rotating the part by angles α and β in x and y axes respectively, is calculated. These values are then normalized to the range of 0 to 1 according to the following function given by Paul and Anand (Paul and Anand, 2014),

$$V_{s\_norm}(\alpha, \beta) = \frac{V_s(\alpha,\beta) - V_{s\_min}}{V_{s\_max} - V_{s\_min}} \quad \dots\dots\dots\dots\dots\dots\dots\dots\dots\dots\dots\dots\dots\dots\dots\dots\dots\dots\dots \ (23)$$

where, $V_s(\alpha,\beta)$ is the volume of support structure at any α and β, V_{s_min} and V_{s_max} is the minimum and maximum volume of support structure at any α and β.

3.5 Combined Optimization for Minimizing Tolerance Errors and Supports

Combining the Cylindricity and Flatness tolerance (Paul and Anand, 2014) with Orientation tolerances, the optimization model to calculate the optimal build angle (α_{opt}, β_{opt}) satisfying all the GD&T callouts while minimizing support structure is given as:

$$\text{Min } E(\alpha, \beta) = \sum_{i=1}^{n_{per}} p_i \omega_i + \sum_{j=1}^{n_{para}} p_j \omega_j + \sum_{k=1}^{n_{ang}} p_k \omega_k + \sum_{l=1}^{n_{cyl}} p_l \omega_l + \sum_{m=1}^{n_{flat}} p_m \omega_m + \omega_s V_{s\_norm} \quad \text{........ (24)}$$

Such that: $0 \leq (c_z^2)_{per}^i \leq (c_{cr1}^2)_{per}^i$, i=1, 2, 3…n_{per}, $0 \leq (c_z^2)_{para}^j \leq (c_{cr3}^2)_{para}^j$, j=1, 2, 3…n_{para},

$0 \leq (c_z^2)_{ang}^k \leq (c_{cr5}^2)_{ang}^k$, k=1, 2, 3…n_{ang}, $(c_{cr}^2)_{cyl}^l \leq (c_z^2)_{cyl}^l \leq 1$, l=1, 2, 3…$n_{cyl}$,

$0 \leq (c_z^2)_{flat}^m \leq (c_{cr}^2)_{flat}^m$, m = 1, 2, 3…n_{flat}, $0° \leq \alpha \leq 360°$, $0° \leq \beta \leq 360°$,

$\sum_{i=1}^{n_{per}} \omega_i + \sum_{j=1}^{n_{para}} \omega_j + \sum_{k=1}^{n_{ang}} \omega_k + \sum_{l=1}^{n_{cyl}} \omega_l + \sum_{m=1}^{n_{flat}} \omega_m + \omega_s = 1$

where, ω_i, ω_j, ω_k, ω_l, ω_m are the weights assigned for perpendicularity, parallelism, angularity, cylindricity, flatness respectively, and ω_s is weight assigned for volume of support structure and p_i are the penalty functions for the respective tolerances that were developed in section 3.3. The weights ensure that the most critical features have the least error. The optimization is formulated as a multivariable minimization problem which has been solved using the fmincon routine available in MATLAB (2013) using the interior-point algorithm (Byrd et al. 1999). It should be noted that fmincon may provide a Pareto optimum solution rather than a global optimum depending on the user defined starting value. If no optimal orientation in which all the GD&T callouts are satisfied is found, either some tolerances have to be loosened or the weights need to be changed. The PMI information extracted from the NX part is utilized in the optimization model to obtain (α_{opt}, β_{opt}), the optimal build angle which the part has to be rotated by to satisfy all the GD&T callouts.

4   Results

The geometric information is extracted using Siemens PLM NX API for the example part shown in Figure 1. The slice thickness is assumed to be 0.06 mm (60 µm). The lower and upper bound for rotating the part is set as 0° to 360° in both x and y directions. Keeping a fixed slice thickness, the weightage given to individual tolerances were varied for different runs. The results attained are tabulated below in Table 1 & Table 2.

Table 1 summarizes the first set of results obtained for the test part which shows the significance of weightages given to support structures (W_{ss}) and tolerances (W_{tol}). The optimization routine generates α_{opt}, β_{opt} which are the angles by which the part has to be rotated about the X and Y axes respectively for the build orientation. In run number 1, 'W_{ss}' was given the maximum weightage (0.4) whereas Perpendicularity was given the highest weight among the tolerances (0.2). The results show that the volume of support structures (V_{ss}) is minimized but Parallelism

Table 1: Results for Optimal Build Orientation

No.	Tols	W_{tol}	W_{ss}	α_{opt}	β_{opt}	V_{ss_opt} (mm³)	Tol callouts	Tol error	
1	Cyl	0.1	0.4	3	46	3.23E+05	0.045	0.0434	✓
	Flat	0.1					0.055	0.0415	✓
	Per	0.2					0.047	0.002	✓
	Para	0.1					0.038	0.0415	✗
	Ang	0.1					0.055	0.0308	✓
2	Cyl	0.05	0.05	31	43	5.19E+05	0.045	0.0814	✗
	Flat	0.05					0.055	0.0321	✓
	Per	0.05					0.047	0.0344	✓
	Para	0.75					0.038	0.0321	✓
	Ang	0.05					0.055	0.0296	✓

which had 10% of the total weightage was not within the callout. Keeping the tolerance callouts constant, weightage given to Parallelism was raised to 75% in the second run. This increment led to a reduced value of Parallelism error which was well within the callout (0.0321 as against 0.0415). Since

weightage given to support structures was reduced from 40% to 5%, an increased value of 'V_{ss}' is reflected in the results (3.23E+05 as against 5.19E+05).

Table 2 summarizes the second set of results obtained for the test part with equal weightage given to all parameters. It was observed that the optimum build angle obtained did not satisfy all the tolerance callouts with the given critical values. A second run was conducted with the same weights but the callout for Parallelism was relaxed. This relaxation led to all the tolerance criteria being satisfied and also reduced the volume of support structures in comparison with the previous run as shown in the Table 2.

To verify the results obtained from the optimization model, an extension of the graphical approach developed by Paul (Paul, 2013) and Paul and Anand (Paul and Anand, 2014) can be adapted for the orientation tolerances as well, as shown in Figure 16.

As a way to visualize the effect of build orientation on meeting the GD&T callouts and the associated support structures volume, the combined information is presented on a unit sphere depicting different build orientations. The part is rotated in increments of 10° and the volume of support structure is found at each orientation. These values are plotted on

Table 2: Results for Optimal Build Orientation

No.	Tols	W_{tol}	W_{ss}	α_{opt}	β_{opt}	V_{ss_opt} (mm³)	Tol callouts	Tol error	
1	Cyl	0.19	0.05	24	41	4.43E+05	0.045	0.0434	✓
	Flat	0.19					0.055	0.0415	✓
	Per	0.19					0.047	0.0181	✓
	Para	0.19					0.038	0.0415	✗
	Ang	0.19					0.055	0.0421	✓
2	Cyl	0.19	0.05	5	35	3.1E+05	0.045	0.0352	✓
	Flat	0.19					0.055	0.0486	✓
	Per	0.19					0.047	0.0045	✓
	Para	0.19					0.057	0.0486	✓
	Ang	0.19					0.055	0.0375	✓

Figure 16: Verification using Graphical Approach

a unit sphere with the color map indicating the amount of support structures required at that particular orientation. As indicated in Figure 17, green represents minimum volume of supports whereas yellow indicates the maximum. It must be noted that the divisions selected in this figure are coarse and for representation only.

Figure 17 explains how this sphere can be used to identify the range of build angle corresponding to each color patch. The center of the sphere lies at the origin of a 3D plane, and 'X', 'Y' and 'Z' represent the different axes. Consider an instance where the user wants to determine the build angle corresponding to the patch marked by the color red on the sphere. The build axis of the part is considered to be the 'Z' axis. Since each of the patches represents a 10 degree range of angle, a rotation of 2 units from 'Z' about the 'X' axis corresponds to a patch having a range of 10° to 20° in the YZ plane. Further rotation by 2 units about the 'Y' axis results in a patch in the range of 10° to 20° in the XZ plane which is the user selected patch.

Figure 17: Determination of angle corresponding to patch

A combined representation of the tolerance values with the corresponding support structures on the unit sphere is shown in Figure 18. The part is rotated in increments of 10^0 and the tolerance error

values are calculated at each of these orientations and checked to see if they are within the tolerance limits.Radial projections are used to represent the number of tolerance callouts satisfied at the respective combination of α and β on the unit sphere as shown in Figure 18. The color of a projection in Figure 18 is decided by the number of tolerances satisfied at that orientation. For example, if at α = 30, β = 10, the number of tolerances satisfied are four, then the color of the projection will be blue. Similarly, black and red projections represent one and two tolerances being satisfied respectively. The figure presented here is a 2D snapshot of an interactive animation that users can readily use for deciphering the effect of a particular build orientation on tolerance callouts and support structures.
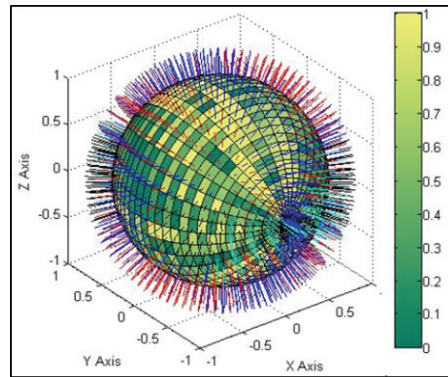

Figure 18: Combined Representation of Support Structures and Tolerances

5   Conclusions and Future Scope

This paper provides an approach for the optimal build orientation which will minimize the volume of support structures while meeting all the GD&T criteria of the part using a weighted optimization approach. Siemens PLM NX API was used to extract the PMI information from the part to calculate the GD&T errors. The volume of support structures was calculated using a Quadtree based approach. The effects of varying the weightage for individual tolerances on the tolerance errors and the volume of support structure were analyzed. This helped in determining which callouts had to be relaxed to obtain required part quality. A combined graphical representation was presented to depict the volume of support structure and the tolerances satisfied at each orientation.

The methodology adopted in this paper can also be extended to include other tolerances such as Runout and Conicity in the optimization model. This approach can also be improved upon to account for effects like warpage and shrinkage arising due to thermal errors. Experimental validation of the results can help in improving the robustness of the model. The unit sphere approach for finding the best build orientations can be interactive to make it more user-friendly and precise.

References

Alexander P, Allen S and Dutta D. Part orientation and build cost determination in layered manufacturing. *Computer Aided Design* 1998; 30(5): 343-356.

Allen S and Dutta D. On the computation of part orientation using support structure in layered manufacturing. *Solid Freeform Fabrication Symposium*, Austin, 1994, pp.259-269.

Arni R and Gupta S. Manufacturability analysis of flatness tolerances in solid freeform fabrication. *Journal Of Mechanical Design* 2001; 123(1): 148-156.

ASME, American National Standards Institute. *Dimensioning and Tolerancing for Engineering Drawings, ANSI Standard Y14.5M* 1994.

Byrd R, Hribar M and Nocedal J. An interior point algorithm for large-scale nonlinear programming. *SIAM Journal on Optimization* 1999; 9(4): 877-900.

Cheng W, Fuh J, Nee A, Wong Y, Loh H and Miyazawa T. Multi objective optimization of part building orientation in stereolithography. *Rapid Prototyping Journal* 1995; 4: 12-23.

Cloots M, Spierings A, and Wegener K. Assessing new support minimizing strategies for the additive manufacturing technology SLM. *Solid Freeform Fabrication Symposium* 2013.

Dutta D and Kulkarni P. A review of process planning techniques in layered manufacturing. *Rapid Prototyping Journal* 2000; 6: 16-35.

Dyer C, Rosenfeld A and Samet H. Region representation: boundary codes from Quadtree. *Commumications of the ACM*, 1980; pp.171-179.

Frank D and Fadel G. Expert system-based selection of the preferred direction of build for rapid prototyping processes. *Journal of Intelligent Manufacturing* 1995; 6(5): 339-345.

Knuth D. *The art of computing volume 3: Sorting & Searching*. Massachusettes: Addison Wesley, 1975.

Lan P, Chou S, Chen L and Gemmill D. Determining fabrication orientations for rapid prototyping with stereolithography apparatus. *Computer Aided Design* 1997; 29(1): 53-62.

Lynn-Charney C and Rosen DW. Usage of accuracy models in stereolithography process planning. *Rapid Prototyping Journal* 2000; 6(2): 77-86.

Majhi J, Janardan R, Schwerdt J, Smid M and Gupta P. Minimizing support structures and trapped area in two-dimensional layered manufacturing. *Comput. Geom.* 1999; 12(3-4): 241-267.

Majhi J, Janardan R, Smid M and Gupta P. On some geometric optimization problems in layered manufacturing. *Comput. Geom.* 1998; 12(3-4): 210-239.

Pandey P, Thrimurthulu K and Venkata Reddy N. Optimal part deposition orientation in FDM by using a multicriteria genetic algorithm. *Int. Journal of Prod. Res.* 2004; 42(19): 4069-4089.

Paul R. Modeling and optimization of powder based additive manufacturing (AM) Processes. Ph.D. Dissertation, University of Cincinnati 2013.

Paul R and Anand S. Optimization of layered manufacturing process for reducing form errors with minimal support structures. doi:10.1016/j.jmsy.2014.06.014, *J. of Manuf. Systems* 2014.

Prakasvudhisarn C and Raman S. Framework for cone feature measurement using coordinate measuring machines. *J. of Manuf. Science* 2004; 1(126): 167-177.

Ramaswami H, Turek S, Rajmohan S and Anand S. A comprehensive methodology for runout tolerance evaluation using discrete data. *Int J of Adv Manuf Technol* 2011; 56(5-8): 663-676.

Rattanawong W, Masood S and Iovenitti P. A volumetric approach to part build orientations in rapid prototyping. *Journal of Materials Processing Technology* 2001; 119(1-3): 348-353.

Samet H. Region representation: Quadtree from binary searches. *Computer Graphics and Image Processing* 1980; 13(1): 88-93.

Samet H. The quadtree and related hierarchical data structures. *ACM Computing Surveys* 1984; 16(2): 187-260.

Samet H and Tamminen M. Computing geometric properties of images represented by linear quadtree. *IEEE Trans. Pattern Analysis Mach. Intell* 1985; *7*(2): 229-240.

Siemens PLM Software. Product and manufacturing information (PMI) management 2009 from http://m.plm.automation.siemens.com/en_us/Images/9645_tcm1224-4581.pdf

Thompson D and Crawford R. Computational quality measures for evaluation of part orientation in freeform fabrication. *Journal Of Manuf. Systems* 1997; 16(4): 273-289.

Thrimurthulu K, Pandey P and Venkata Reddy N. Optimum part deposition orientation in fused deposition modeling. *Int. Journal of Machine Tools and Manufacture* 2004; 44(6): 585-594.

Wen X, Huang J, Wang F and Sheng D. Conicity and cylindricity error evaluation using particle swarm optimization. *Precision Engineering* 2010; 34(2): 338-344.

Xu F, Wong Y, Loh H, Fuh J and Miyawaza T. Optimal orientation with variable slicing in stereolithography. *Rapid Prototyping Journal* 1997; 3(3): 76-88.

Yang Y, Fuh J, Loh H and Wong Y. Multi-orientational deposition to minimize support in the layered manufacturing process. *Journal of Manuf. Systems* 2003; 22(2): 116-129.

Zhang J and Li Y. A unit sphere discretization and search approach to optimize building direction with minimized volumetric error for rapid prototyping. *Int J of Adv Manuf Technol* 2013; 67(1-4): 733-743.